CONSIDERATIONS OF METHODS OF IMPROVING

HELICOPTER EFFICIENCY

By Richard C. Dingeldein

Langley Research Center

SUMMARY

Recent NASA helicopter research indicates that significant improvements in hovering efficiency, up to 7 percent, are available from the use of the NACA 63A015(230) airfoil section. This airfoil should be considered for flying-crane-type helicopters. Application of standard leading-edge roughness causes a large drop in efficiency; however, the cambered rotor is shown to retain its superiority over a rotor having a symmetrical airfoil when both rotors have leading-edge roughness.

A simple analysis of available rotor static-thrust data indicates a greatly reduced effect of compressibility effects on the rotor profile-drag power than predicted from calculations.

Preliminary results of an experimental study of helicopter parasite drag indicate the practicability of achieving an equivalent flat-plate parasite-drag area of less than 4 square feet for a rotor-head—pylon—fuselage configuration (landing gear retracted) in the 2,000-pound minimum-flying-weight class. The large drag penalty of a conventional skid-type landing (3.6 square feet) can be reduced by two-thirds by careful design. Clean, fair, and smooth fuselages that tend to have narrow, deep cross sections are shown to have advantages from the standpoint of drag and download. A ferry range of the order of 1,500 miles is indicated to be practicable for the small helicopter considered.

INTRODUCTION

This paper summarizes the results of recent research relating to improving the efficiency of a helicopter in hovering and in forward flight. The reader having competence in the field of helicopter aerodynamics will recognize no new or startling concepts. The data presented, however, are believed to assure the practicability of large helicopter performance improvements.

Large gains in rotor hovering efficiency are shown for a special airfoil formed by combining an NACA 6A-series thickness distribution and an NACA forward-camber mean line. The reduction in efficiency accompanying two different conditions of rotor-blade leading-edge roughness is given. Available static-thrust data obtained on a large number of helicopter rotors operated at high tip speeds are summarized to show the general effect of compressibility on the rotor profile-drag power coefficient and are compared with calculated predictions. In addition, preliminary results obtained from an experimental study of helicopter parasite drag are presented to show the relative drag of the different helicopter components. This information forms the basis of calculations used to demonstrate significant improvements in helicopter cruising efficiency.

SYMBOLS

b	number of rotor blades
c	blade chord at station x

c_e equivalent blade chord, $\dfrac{\displaystyle\int_0^1 cx^2 dr}{\displaystyle\int_0^1 x^2 dr}$

D	parasite drag, lb
L	lift, lb
T	rotor thrust, lb
M	Mach number
P	rotor power, $\dfrac{\text{ft-lb}}{\text{sec}}$
R	rotor radius, ft
C_T	rotor thrust coefficient, $\dfrac{T}{\rho(\Omega R)^2 \pi R^2}$
C_P	rotor power coefficient, $\dfrac{P}{\rho(\Omega R)^3 \pi R^2}$

$\overline{C}_L$ rotor mean lift coefficient, $\dfrac{6C_T}{\sigma}$

r   radius to blade element, ft

x = r/R

SFC   specific fuel consumption, lb/hp-hr

α angle of attack

ρ density of air, slugs/cu ft

Ω rotor angular velocity, radians/sec

σ rotor solidity, $\dfrac{bc_e}{\pi R}$

θ_1 rotor-blade geometric twist (negative sign denotes washout), deg

Subscripts:

0   profile drag

t   blade tip

div   denotes drag divergence of two-dimensional airfoil

f   fuselage

RESULTS AND DISCUSSION

Hovering Efficiency

Effect of camber.- The advantages of cambered rotor blades in respect to producing improved hovering and forward-flight efficiency are well known. (See refs. 1 to 3.) In an effort to define a rotor-blade airfoil section that would essentially realize the largest practicable gains in hovering efficiency that are available through airfoil selection, an NACA 63A015 thickness distribution was mated to an NACA 230 mean line. This thickness distribution was chosen because helicopter tower tests of a rotor having an NACA 63_2-015 airfoil section (ref. 4) indicated the highest overall combination of high maximum mean rotor lift coefficients and resistance to compressibility drag rise of a number

of full-scale rotors previously tested. The NACA 63A015 thickness distribution should have essentially the same aerodynamic characteristics as the NACA 63_2-015 thickness distribution (refs. 5 and 6) and its larger trailing-edge angle avoids construction problems associated with the cusped trailing edge. The expectation, then, was to realize the benefits of camber without introducing large quarter-chord pitching moments or early drag divergence. Rotor blades having the new airfoil (denoted as the NACA 63A015(230)) were tested on the Langley helicopter tower (ref. 7). A sample of the results is shown in figure 1, in which the rotor hovering efficiency (defined as the rotor figure of merit) is plotted against the rotor-blade tip Mach number for values of the rotor mean lift coefficient $\bar{C}_L$ of 0.5, 0.7, and 0.9. This parameter is proportional to the rotor-blade loading. A utility helicopter would probably operate at the lower value shown, a flying-crane type at the higher values. Also shown are the data for the rotor having an NACA 63_2-015 airfoil section. These rotors were similar in respect to solidity, twist, and surface condition. Substantial gains due to camber, up to 6 or 7 percentage points, are indicated. At typical rotor disk loadings, a 5-percent gain in figure of merit is equivalent to an extra one-half to two-thirds of a pound of rotor thrust per horsepower delivered to the rotor. This value is equivalent to a 5- to 8-percent increase in the gross rotor thrust, or a 10- to 15-percent or more increase in the helicopter payload. The gains due to camber disappear as the rotor-tip Mach number increases past 0.6; however, this is not a range generally associated with a flying-crane helicopter.

It should be noted that the gains indicated in figure 1 did not require extreme care with the airfoil contour and surface condition. For example, the high efficiencies shown in figure 1 do not depend on a section drag polar having the familiar bucket shape. The contour was good and the blades were smooth and fair, but no elaborate quality-control procedures were taken.

It should also be stated that the data shown for the NACA 63_2-015 rotor average some 2- to 4-percent higher hovering efficiencies than were obtained on the helicopter tower from tests of a rotor having the widely used NACA 0012 airfoil.

Effect of leading-edge roughness.- Since rotor blades may not be operated in the smooth condition due to the abrading effects of field operation, two different amounts of leading-edge roughness were investigated. First, shellac of rather thick consistency was applied over an area extending 8 percent of the chord (measured along the surface) back from the leading edge on both the upper and lower surfaces. The resulting spanwise brush marks produced surface waves 0.002 to 0.004 inch in height. Next, the aforementioned condition was removed and NACA standard

leading-edge roughness was added. This roughness consisted in applying fresh shellac over the same area previously described and sprinkling with 0.005-inch grains of carborundum distributed to cover about 5 percent of the area. Measurements of the typical roughness heights showed variations from about 0.006 inch to 0.009 inch. The resulting hovering efficiencies are compared with the smooth rotor in figure 2. The shellac alone had very little effect, but the standard roughness caused up to a 12- or 13-percent drop in the hovering efficiency. This decrease in hovering efficiency, of course, corresponds to a similar increase in the power required to produce a given rotor thrust. The high hovering efficiency capabilities of the NACA 63A015(230) airfoil, therefore, cannot be expected unless the rotor blades are built and kept fairly smooth. The condition of NACA standard leading-edge roughness is believed comparable to the severe erosion that has already been noted in certain helicopter operations and with present blade leading-edge materials.

In figure 3 is shown a comparison between the rotors having NACA 63A015(230) and NACA 63_2-015 airfoil sections for the condition of NACA standard roughness applied to both rotors. It is seen that the cambered airfoil retains its considerable superiority in hovering efficiency over the range of test conditions presented.

Effect of reduced thickness and camber.- In an attempt to improve rotor hovering efficiency at rotor tip Mach numbers above 0.6 while retaining some of the advantages indicated for camber at the lower rotor tip Mach numbers, the NACA 63A012 thickness distribution was mated to an NACA 130 mean line. The results of testing a rotor having the resulting NACA 63A012(130) airfoil are shown in figure 4. The combined effects of reduced thickness and camber are seen to give reduced hovering efficiency compared with the NACA 63A015(230) rotor at $\overline{C}_L = 0.9$ and 0.7, and gains at $\overline{C}_L = 0.5$ only at the higher blade tip Mach numbers. For the range of conditions illustrated in figure 4, the NACA 63A012(130) rotor nevertheless indicates somewhat higher efficiencies than the NACA 63_2-015 rotor. It is believed that the NACA 63A015(230) airfoil represents as good a compromise for a load-lifter type helicopter as can be obtained from the standpoint of airfoil choice.

Effect of compressibility on rotor power requirements.- The preceding discussion of figures 1 and 3 has touched on the reduced hovering efficiency associated with the higher rotor-blade tip Mach numbers. From the standpoint of achieving higher forward speeds, the use of higher rotor tip speeds continues to be of interest. A number of large-scale helicopter rotors have been tested in static thrust at relatively high blade-tip Mach numbers, mostly on the Langley helicopter tower facility. (See, for example, refs. 4 and 8 to 11.) A summary of the test results, representing rotor-blade airfoil sections from 6 to 18 percent thick

and rotational blade-tip Mach numbers as high as 1, is shown in figure 5.
The purpose of this figure is not to compare airfoils but to provide a
quick, broad look at the overall effect of compressibility on the rotor
hovering-power requirements. In an attempt to generalize the results,
increments in the rotor profile-drag power coefficient measured over the
available ranges of rotor tip Mach number and blade pitch angle afforded
by the test data were divided by the rotor solidity and plotted against
the amount by which the rotor-blade tip Mach number exceeded the drag-
divergence Mach number determined from two-dimensional airfoil tests.
Also shown is a shaded area representing the results of a number of strip
calculations for two different NACA 0012 rotors using compressible air-
foil section data and covering a range of blade pitch and tip Mach number.
The experimental data are seen to group in a band that lies well below the
calculated predictions. A substantial tip relief is also indicated. It
therefore appears that greatly reduced effects of compressibility on the
power required in forward flight were experienced compared with calcu-
lated estimates. The most serious effects of compressibility are prob-
ably associated with blade and rotor stability problems; however, these
results can be considered as somewhat encouraging. This general research
area requires more study.

Cruising Efficiency

Improvements in the forward-flight efficiency of helicopters, pri-
marily with respect to cruising speed and range, are being sought by
helicopter operators, particularly the military. Obtaining these
improvements is mainly dependent upon the reduction of parasite drag.
(See, for example, refs. 12 and 13; the powerplant installation is
treated in ref. 14.) In the remainder of the paper the problem will be
examined and the preliminary results of recent research will be dis-
cussed and used to illustrate the practicability of achieving significant
improvements in helicopter forward-flight efficiency, particularly the
ferry range.

Parasite drag.- There is considerable airplane-drag—cleanup experi-
ence to profit from. (See refs. 15 to 20.) However, the rotor-head—
pylon—fuselage combination and the presence of potentially large fuse-
lage downloads in hovering and in forward flight constitute problems
peculiar to rotating-wing aircraft and hence warrant special study. An
experimental model and full-scale test program has been initiated to study
means of achieving low helicopter drag and to assess the drag penalties of
various helicopter components. The model tests, conducted at 1/5 scale
in the Langley 300-MPH 7- by 10-foot tunnel at a dynamic pressure of about
210 pounds per square foot, are primarily aimed at studying the effect of
fuselage and pylon shape and to establish the primary problem areas. The
full-scale tunnel test provides data essentially free of scale effects and
permits the evaluation of actual hardware, such as antennas.

Sketches of the four model fuselage shapes tested are given in figure 6. Shapes A and B had narrow, deep cross sections in an attempt to reduce downloads in hovering and forward flight, as well as the drag variation with fuselage attitude. The other two shapes had only slightly oval cross sections forward. Shape D had a fairly constant-width forebody terminating in a rather abrupt narrowing of the planform aft of the cabin. The model fuselages were approximately 5 feet long. The projected frontal areas of shapes A, B, C, and D were, respectively, 0.75 square foot, 0.71 square foot, 0.75 square foot, and 0.75 square foot.

Sample equivalent flat-plate parasite-drag areas obtained for fuselage shape C and for a pylon, rotating rotor head, and two different skid-type landing gears are shown in figure 7 for a fuselage angle of attack of 0°. No support-interference corrections have been applied. The model data have been scaled up to the full-scale values, which, in this case, can be taken as representative of a helicopter having a minimum flying weight of the order of 2,000 pounds. The drag of the basic smooth, clean, and fair fuselage is 1 square foot. Adding a clean, streamlined pylon brings the total to 3 square feet. Adding an estimated allowance for the tail rotor brings the total to 3.5 square feet. Installing a conventional skid landing gear of tubular construction doubles the parasite drag to a value of 7.1 square feet. A skid gear which is designed for low drag by using streamlined support struts that track at the cruise attitude and intersect the fuselage normal to the surface rather than at an acute angle is seen to add only about one-third the drag of the conventional gear for a total helicopter parasite-drag area of 4.7 square feet. The literature (refs. 18 to 20) indicates a similar increment from a clean wheel-type gear. The penalty for a dirty-wheel arrangement can be several times this increment. The data provide good arguments for cleaning up or completely retracting the landing gear of a high-performance helicopter.

The Reynolds number of the tubular gear, based on the cylinder diameter, was below the critical value for the model tests. A consideration of the full-scale landing gear that it was patterned after indicates that it, too, would be below the critical Reynolds number for cruising speeds below 110 knots.

The fuselage and pylon parasite-drag values shown are not at all representative of current helicopters, which customarily penalize an already poor aerodynamic shape with additional drag from leakage and nonflush doors, windows, hatches, and other protuberances which not only contribute their own drag but also cause flow separation on the basic fuselage.

Additional preliminary lift and drag data obtained from the 1/5-scale model tests are given in figures 8 and 9. From figure 8 it is seen

that minimum equivalent flat-plate parasite-drag areas of fuselage shapes A and C of the order of 1 square foot were measured. Shapes B and D indicate progressively higher minimum drag, which is probably the result of flow separation in the vicinity of the tail-boom juncture and the abrupt planform closure, respectively. The advantages of a fuselage shape that tends to be narrow and deep rather than broad in cross section is clearly shown in figure 8. Greatly reduced downloads are indicated for fuselages A and B at typical forward-flight attitudes compared with fuselages C and D. Reduced downloads in hovering would also be expected for shapes A and B. Somewhat more favorable variation in the fuselage drag with angle of attack is also apparent. The fact that two of the four fuselages showed relatively low drag, somewhat higher drag being indicated for the two shapes (B and D) that were more subject to flow separation, indicates the importance of designing a smooth and fair shape that avoids sudden changes in contour if low parasite drag is to be achieved. Improved aircraft-construction practice similar to that used on high-performance conventional aircraft will be necessary.

The increase in parasite drag with angle of attack noted in figure 9 (about 1/2 square foot in going from $\alpha_f = 0^\circ$ to $\alpha_f = -5^\circ$) constitutes a performance penalty. Improved cruising efficiency can be obtained by installing the rotor shaft at an angle in order to keep the fuselage level in cruise.

A consideration of area and volume relationships indicates that it should be considerably less difficult to achieve a proportionately low parasite drag for heavier helicopters.

Ferry-range capability.- In order to determine a practicable ferry range for a clean turbine-powered helicopter of the type for which the previously presented drag data were obtained, limited performance estimates were made with available calculation procedures. (See refs. 21 to 23.) An equivalent parasite-drag area of 4 square feet, which assumes a retractable landing gear, was used. Also selected were a rotor solidity of 0.07, a blade twist of -8°, and a design rotor tip speed of 600 feet per second. These parameters were selected to provide good overweight performance. Calculations of the cruise performance were made over a range of gross weights. The maximum effective helicopter lift-drag ratios calculated, which occur at airspeeds of the order of 110 knots, are plotted in figure 10 over a range of ratios of gross weight to normal gross weight. The overload for the ferry mission would be primarily fuel. An L/D of about 7 is indicated at weight ratios above 1.4, which, incidentally, would require a running take-off. Reduced efficiency is indicated at normal gross weight, although the clean helicopter is seen to show to advantage over current practice. A flight procedure of gradually reducing the speed of the power turbine to 85-percent rated speed at the

normal gross weight has the effect of producing an almost constant value of L/D of 7 over the broad range of weight ratios shown.

By using a conservative average L/D of 6, a specific fuel consumption of 0.75 lb/hp-hr, and a minimum flying weight of 1,950 pounds (includes pilot and 1 crew), the ferry-range potential shown in figure 11 is calculated. The Breguet range equation was used; the results were multiplied by a 70-percent factor to allow for take-off, climb, headwinds, and fuel reserves. For a running take-off with 2,000 pounds of fuel on-board, a ferry range of 1,500 miles is indicated. The assumptions of this analysis are believed to be realistic, if not conservative.

CONCLUDING REMARKS

Considerations of the results of recent NASA helicopter research programs have indicated the practicability of large improvements in rotor hovering efficiency by the use of a smooth NACA 63A015(230) rotor airfoil section. Increases in the rotor figure of merit as high as 6 or 7 percent have been demonstrated over an improved rotor having symmetrical airfoil sections. Leading-edge roughness of the type that has been experienced in some helicopter operations is shown to reduce the hovering efficiency drastically. The gains associated with camber, however, are retained over the symmetrical airfoil with standard leading-edge roughness applied. The advantages of camber in this particular case tended to disappear above rotor-blade tip Mach numbers of 0.6.

A simple presentation of available helicopter rotor hovering data obtained over a broad range of airfoil sections, blade-tip Mach numbers, and pitch angles indicates greatly reduced rotor profile-drag power losses due to compressibility effects than predicted by calculations.

Preliminary results of a model study of helicopter parasite drag indicate the importance of using clean, fair, and smooth fuselage shapes if low drag is to be achieved. The use of fuselage cross sections that tend to be narrow and deep is shown to give a lower drag variation with angle of attack and greatly reduced downloads. The importance of cleaning up or completely retracting the landing gear is demonstrated. Equivalent total flat-plate parasite-drag areas of 7.1 square feet, 4.7 square feet, and 3.5 square feet are indicated for a full-scale helicopter (minimum flying weight of the order of 2,000 pounds) equipped with conventional skid gear, a low-drag skid gear, and a retractable gear, respectively. A ferry-range capability of 1,500 miles is estimated.

REFERENCES

1. Gustafson, F. B.: Effect on Helicopter Performance of Modifications in Profile-Drag Characteristics of Rotor-Blade Airfoil Sections. NACA WR L-26, 1944. (Formerly NACA ACR L4H05.)

2. Schaefer, Raymond F., and Smith, Hamilton A.: Aerodynamic Characteristics of the NACA 8-H-12 Airfoil Section at Six Reynolds Numbers from 1.8×10^6 to 11.0×10^6. NACA TN 1998, 1949.

3. McCloud, John L., III, and McCullough, George B.: Wind-Tunnel Tests of a Full-Scale Helicopter Rotor With Symmetrical and With Cambered Blade Sections at Advance Ratios From 0.3 to 0.4. NACA TN 4367, 1958.

4. Shivers, James P., and Carpenter, Paul J.: Experimental Investigation on the Langley Helicopter Test Tower of Compressibility Effects on a Rotor Having NACA 63_2-015 Airfoil Sections. NACA TN 3850, 1956.

5. Loftin, Laurence K., Jr.: Theoretical and Experimental Data for a Number of NACA 6A-Series Airfoil Sections. NACA Rep. 903, 1948. (Supersedes NACA TN 1368.)

6. Lindsey, W. F., and Humphreys, Milton D.: Tests of the NACA 64_1-012 and 64_1A012 Airfoils at High Subsonic Mach Numbers. NACA RM L8D23, 1948.

7. Shivers, James P.: Hovering Tests of a Rotor Having an Airfoil Section Especially Suited for Flying-Crane Type Helicopters. (Prospective NASA paper.)

8. Jewel, Joseph W., Jr., and Harrington, Robert D.: Effect of Compressibility on the Hovering Performance of Two 10-Foot Diameter Helicopter Rotors Tested in the Langley Full-Scale Tunnel. NACA RM L58B19, 1958.

9. Carpenter, Paul J.: Lift and Profile-Drag Characteristics of an NACA 0012 Airfoil Section as Derived From Measured Helicopter-Rotor Hovering Performance. NACA TN 4357, 1958.

10. Shivers, James P., and Carpenter, Paul J.: Effects of Compressibility on Rotor Hovering Performance and Synthesized Blade-Section Characteristics Derived From Measured Rotor Performance of Blades Having NACA 0015 Airfoil Tip Sections. NACA TN 4356, 1958.

11. Shivers, James P.: High-Tip-Speed Static-Thrust Tests of a Rotor Having NACA 63(215)A018 Airfoil Sections With and Without Vortex Generators Installed. NASA TN D-376, 1960.

12. Harrington, Robert D.: Reduction of Helicopter Parasite Drag. NACA TN 3234, 1954.

13. Churchill, Gary B., and Harrington, Robert D.: Parasite-Drag Measurements of Five Helicopter Rotor Hubs. NASA MEMO 1-31-59L, 1959.

14. Henry, John R.: Aspects of Internal-Flow-System Design for Helicopter Propulsive Units. NACA RM L54F29, 1954.

15. Dearborn, C. H., and Silverstein, Abe: Drag Analysis of Single-Engine Military Airplane Tested in the NACA Full-Scale Wind Tunnel. NACA WR L-489, 1940. (Formerly NACA ACR, Oct. 1940.)

16. Lange, Roy H.: A Summary of Drag Results From Recent Langley Full-Scale-Tunnel Tests of Army and Navy Airplanes. NACA WR L-108, 1945. (Formerly NACA ACR L5A30.)

17. Bierman, David, and Herrnstein, William H., Jr.: The Interference Between Struts in Various Combinations. NACA Rep. 468, 1933.

18. Herrnstein, William H., Jr., and Bierman, David: The Drag of Airplane Wheels, Wheel Fairings, and Landing Gears - I. NACA Rep. 485, 1934.

19. Bierman, David, and Herrnstein, William H., Jr.: The Drag of Airplane Wheels, Wheel Fairings, and Landing Gears. II - Nonretractable and Partly Retractable Landing Gears. NACA Rep. 518, 1935.

20. Herrnstein, William H., Jr., and Bierman, David: The Drag of Airplane Wheels, Wheel Fairings, and Landing Gears - III. NACA Rep. 522, 1935.

21. Gessow, Alfred, and Tapscott, Robert J.: Charts for Estimating Performance of High-Performance Helicopters. NACA Rep. 1266, 1956. (Supersedes NACA TN 3323 by Gessow and Tapscott and TN 3482 by Tapscott and Gessow.)

22. Gustafson, F. B., and Gessow, Alfred: Effect of Blade Stalling on the Efficiency of a Helicopter Rotor As Measured in Flight. NACA TN 1250, 1947.

23. Gessow, Alfred, and Crim, Almer D.: A Theoretical Estimate of the Effects of Compressibility on the Performance of a Helicopter Rotor in Various Flight Conditions. NACA TN 3798, 1956.

EFFECT OF CAMBER ON HOVERING EFFICIENCY

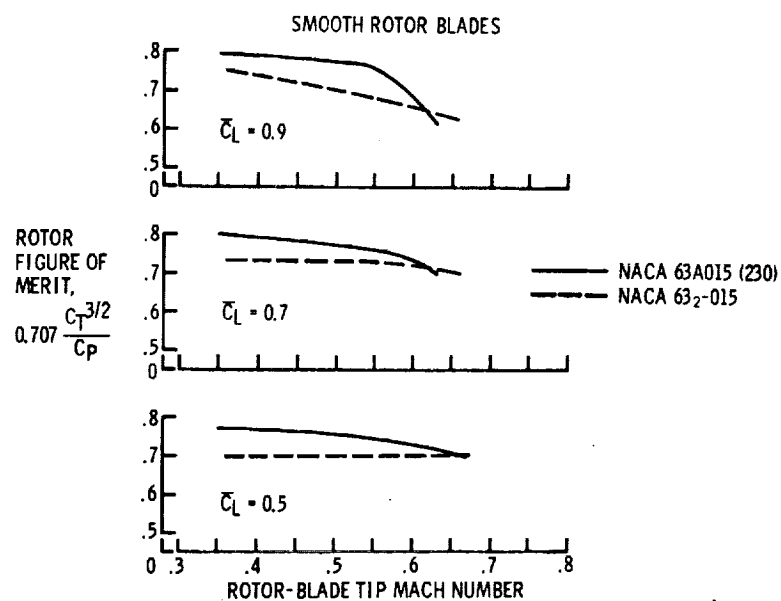SMOOTH ROTOR BLADES

ROTOR FIGURE OF MERIT,

$$0.707 \frac{C_T^{3/2}}{C_P}$$

$\overline{C}_L = 0.9$

$\overline{C}_L = 0.7$

——— NACA 63A015 (230)
– – – NACA 63_2-015

$\overline{C}_L = 0.5$

.8
.7
.6
.5
0

.8
.7
.6
.5
0

.8
.7
.6
.5

0 .3 .4 .5 .6 .7 .8
ROTOR-BLADE TIP MACH NUMBER

Figure 1

EFFECT OF ROUGHNESS ON HOVERING EFFICIENCY

$\overline{C}_L = 0.9$

CONDITION OF LEADING EDGE

——— SMOOTH
– – – SHELLAC WITH BRUSH MARKS
- - - - STANDARD ROUGHNESS

ROTOR FIGURE OF MERIT,

$$0.707 \frac{C_T^{3/2}}{C_P}$$

$\overline{C}_L = 0.7$

$\overline{C}_L = 0.5$

.8
.7
.6
.5
0

.8
.7
.6
.5
0

.8
.7
.6
.5

0 .3 .4 .5 .6 .7 .8
ROTOR-BLADE TIP MACH NUMBER
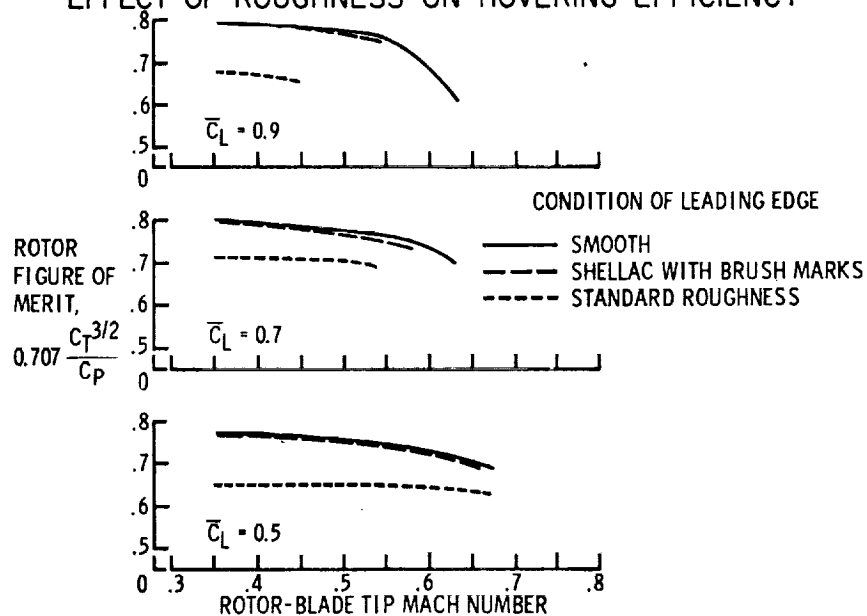
Figure 2

EFFECT OF CAMBER ON HOVERING EFFICIENCY
(NACA STANDARD L.E. ROUGHNESS)

ROTOR FIGURE OF MERIT,

$$0.707 \frac{C_T^{3/2}}{C_P}$$

NACA 63A015 (230)
NACA 63_2 - 015

$\overline{C}_L = 0.9$

$\overline{C}_L = 0.7$

$\overline{C}_L = 0.5$

ROTOR-BLADE TIP MACH NUMBER
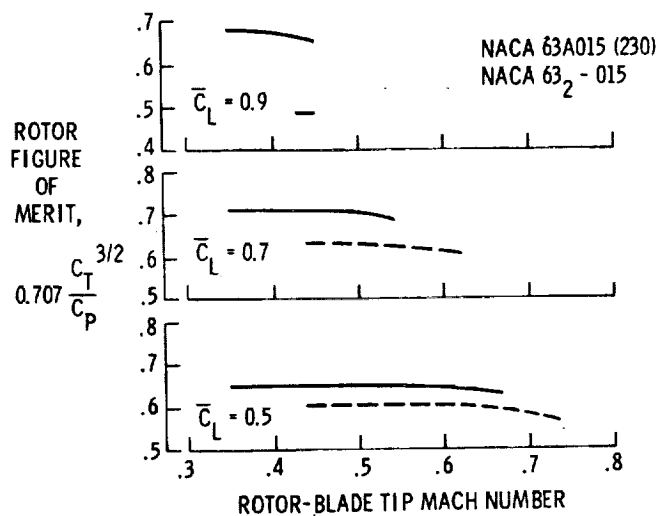
Figure 3

EFFECT OF AIRFOIL SECTION ON HOVERING EFFICIENCY

ROTOR FIGURE OF MERIT,

$$0.707 \frac{C_T^{3/2}}{C_P}$$

$\overline{C}_L = 0.9$

$\overline{C}_L = 0.7$

NACA 63A015 (230)
NACA 63A012 (130)

$\overline{C}_L = 0.5$

ROTOR-BLADE TIP MACH NUMBER
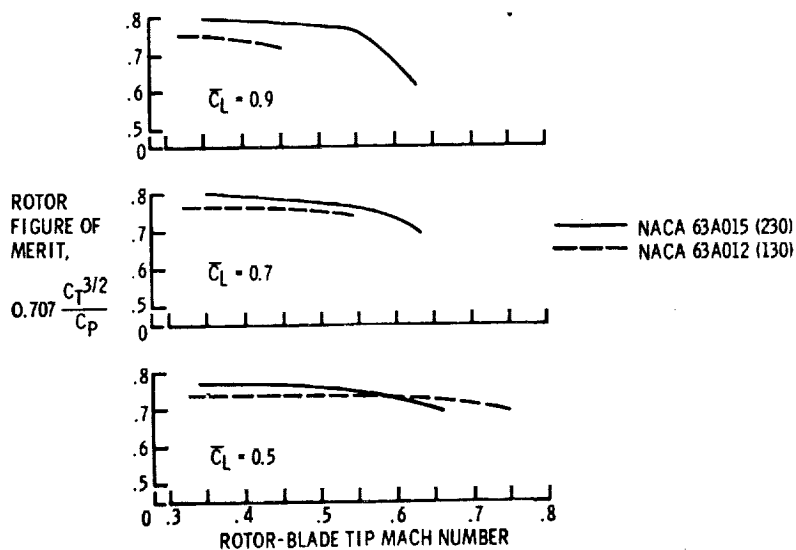
Figure 4

COMPRESSIBILITY EFFECTS ON HOVERING HELICOPTER ROTORS

ROTOR AIRFOIL SECTION

○ NACA 64-006
□ 0012
◇ 0015
△ 63_2-015
◊ $63_{(215)}$A018

$\dfrac{\Delta C_{P,0}}{\sigma}$

CALCULATED

MEASURED

$M_t - M_{DIV}$
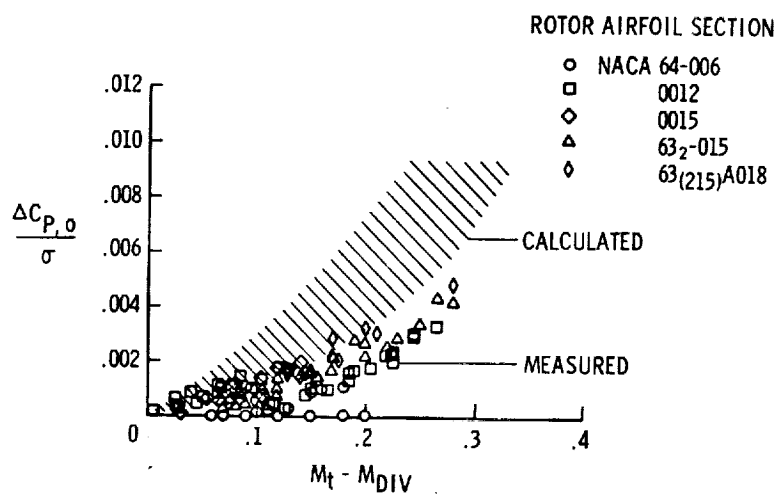
Figure 5

FUSELAGE SHAPES USED IN MODEL TESTS

A

B

D

C
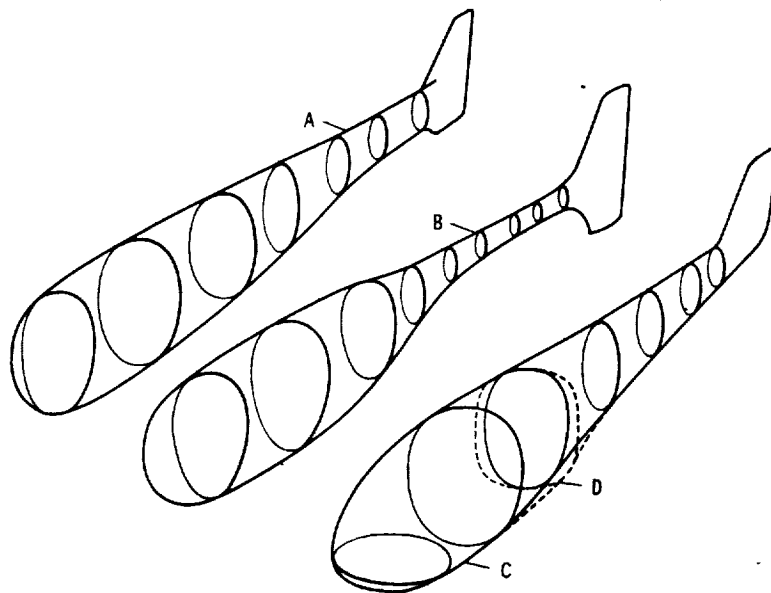
Figure 6

EQUIVALENT PARASITE DRAG AREAS OF
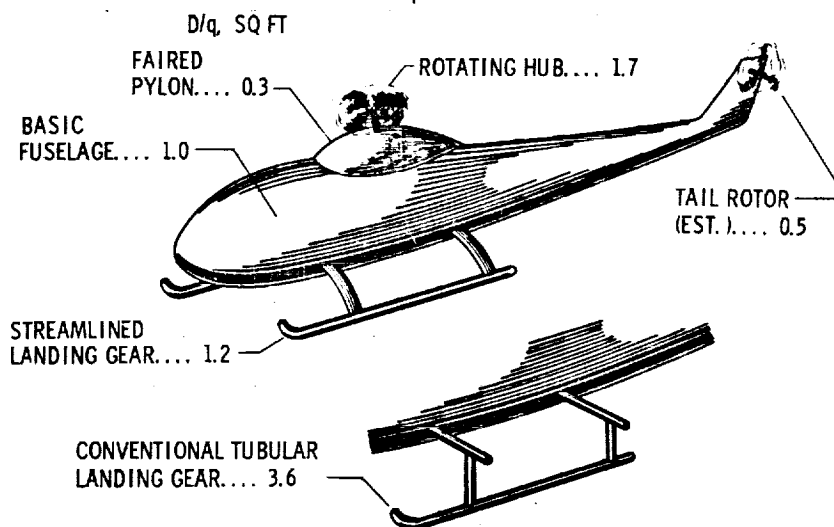VARIOUS HELICOPTER COMPONENTS

$\alpha_f = 0^0$

D/q, SQ FT

FAIRED PYLON.... 0.3

ROTATING HUB.... 1.7

BASIC FUSELAGE.... 1.0

TAIL ROTOR (EST.).... 0.5

STREAMLINED LANDING GEAR.... 1.2

CONVENTIONAL TUBULAR LANDING GEAR.... 3.6

Figure 7

LIFT AND DRAG CHARACTERISTICS OF
BASIC FUSELAGE SHAPES
(MODEL DATA PRESENTED FOR FULL-SCALE HELICOPTER)

$\frac{D}{q}$, SQ FT

$\frac{L}{q}$, SQ FT
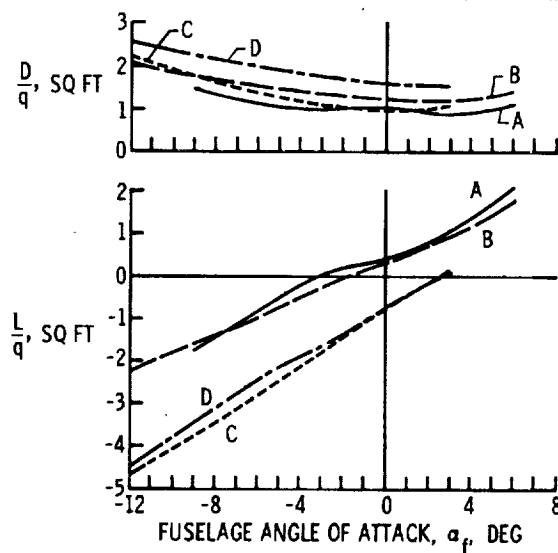
FUSELAGE ANGLE OF ATTACK, α_f, DEG

Figure 8

SAMPLE MODEL FUSELAGE DRAG DATA

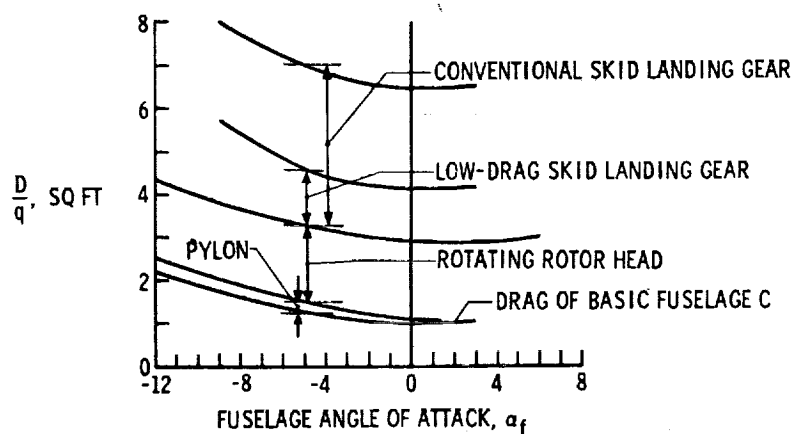### RESULTS PRESENTED FOR FULL-SCALE HELICOPTER

Figure 9

LIFT—DRAG RATIOS CALCULATED FOR SAMPLE HELICOPTER

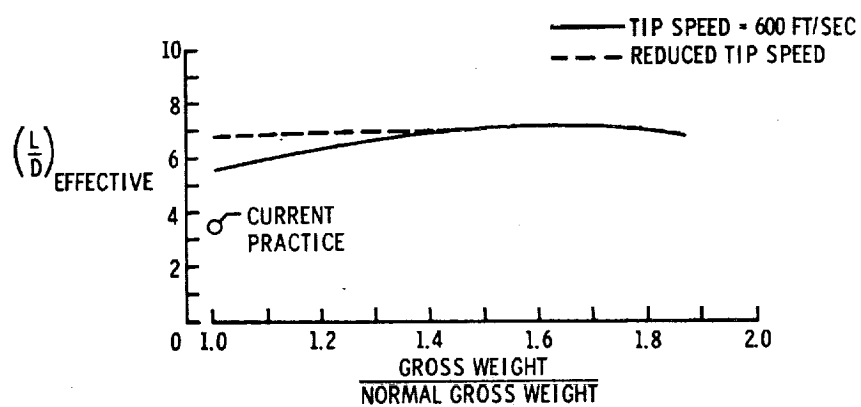$$\sigma = 0.07; \frac{D}{q} = 4 \text{ SQ FT}; \theta_1 = -8^0$$
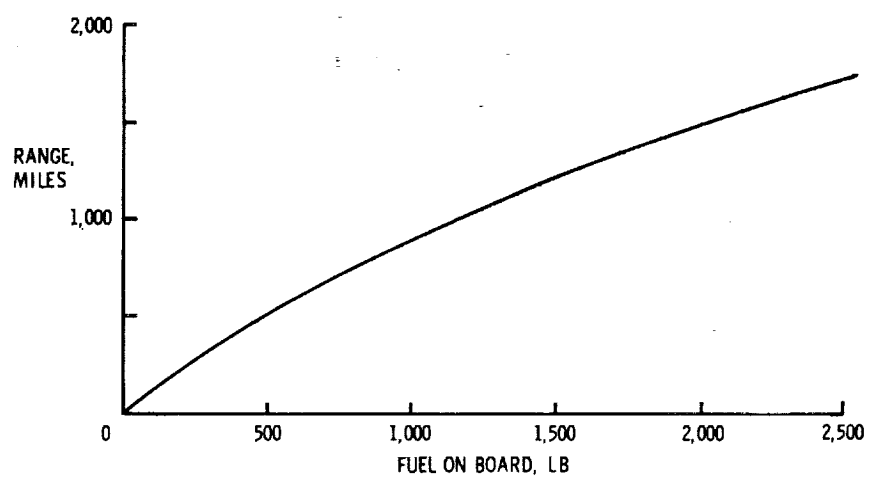

Figure 10

FERRY RANGE POTENTIAL

$\frac{L}{D}$ = 6; SFC = 0.75 LB/HP-HR; MINIMUM FLYING WEIGHT = 1,950 LB

Figure 11